



Deleterious genetic changes in *AGTPBP1* result in teratozoospermia with sperm head and flagella defects

Yu-Hua Lin^{1,2} | Ya-Yun Wang³ | Tsung-Hsuan Lai^{4,5} | Jih-Lung Teng³ | Chi-Wei Lin³ |
Chih-Chun Ke⁶ | I-Shing Yu⁷ | Hui-Ling Lee² | Chying-Chyuan Chan⁸ |
Chi-Hua Tung⁹  | Donald F. Conrad¹⁰ | Moira K. O'Bryan¹¹ | Ying-Hung Lin³ 

¹Division of Urology, Department of Surgery, Cardinal Tien Hospital, New Taipei, Taiwan

²Department of Chemistry, Fu Jen Catholic University, New Taipei City, Taiwan

³Graduate Institute of Biomedical and Pharmaceutical Science, Fu Jen Catholic University, New Taipei City, Taiwan

⁴Department of Obstetrics and Gynecology, Cathay General Hospital, Taipei, Taiwan

⁵School of Medicine, Fu Jen Catholic University, New Taipei City, Taiwan

⁶Department of Urology, En Chu Kong Hospital, New Taipei City, Taiwan

⁷Laboratory Animal Center, College of Medicine, National Taiwan University, Taipei, Taiwan

⁸Department of Obstetrics and Gynecology, Taipei City Hospital, Zhongxing Branch and Branch for Women and Children, Taipei, Taiwan

⁹Program of Artificial Intelligence & Information Security, Fu Jen Catholic University, New Taipei City, Taiwan

¹⁰Division of Genetics, Oregon National Primate Research Center, Beaverton, Oregon, USA

¹¹School of BioSciences and Bio21 Institute, The University of Melbourne, Parkville, Victoria, Australia

Correspondence

Ying-Hung Lin, Graduate Institute of Biomedical and Pharmaceutical Science, Fu Jen Catholic University, New Taipei City, Taiwan.

Email: 084952@mail.fju.edu.tw

Funding information

Cardinal Tien Hospital, Grant/Award Number: CTH-112A-2209; Ministry of Science and Technology of the Republic of China, Grant/Award Number: MOST 109-2320-B-030-002-; MOST 110-2320-B-030-002-; National Science and Technology Council in Taiwan, Grant/Award Number: NSTC 111-2320-B-030-007-MY3

Abstract

Approximately 10%–15% of couples worldwide are infertile, and male factors account for approximately half of these cases. Teratozoospermia is a major cause of male infertility. Although various mutations have been identified in teratozoospermia, these can vary among ethnic groups. In this study, we performed whole-exome sequencing to identify genetic changes potentially causative of teratozoospermia. Out of seven genes identified, one, *ATP/GTP Binding Protein 1* (*AGTPBP1*), was characterized, and three missense changes were identified in two patients (Affected A: p.Glu423Asp and p.Pro631Leu; Affected B: p.Arg811His). In those two cases, severe sperm head and tail defects were observed. Moreover, *AGTPBP1* localization showed a fragmented pattern compared to control participants, with specific localization in the neck and annulus regions. Using murine models, we found that *AGTPBP1* is localized in the manchette structure, which is essential for sperm structure formation. Additionally, in *Agtpbp1*-null mice, we observed sperm head and tail defects similar to those in sperm from *AGTPBP1*-mutated cases, along with abnormal polyglutamylation tubulin and decreasing Δ -2 tubulin levels. In this study, we established a link between genetic changes in

Yu-Hua Lin and Ya-Yun Wang were authors contributed equally to this work.

This is an open access article under the terms of the [Creative Commons Attribution](https://creativecommons.org/licenses/by/4.0/) License, which permits use, distribution and reproduction in any medium, provided the original work is properly cited.

© 2023 The Authors. *Journal of Cellular and Molecular Medicine* published by Foundation for Cellular and Molecular Medicine and John Wiley & Sons Ltd.

AGTPBP1 and human teratozoospermia for the first time and identified the role of *AGTPBP1* in deglutamination, which is crucial for sperm formation.

KEYWORDS

AGTPBP1, genetic changes, male infertility, teratozoospermia, whole-exome sequencing

1 | INTRODUCTION

Infertility has been recognized as a global public health concern by the World Health Organization (WHO), and affects at least 8%–12% of couples worldwide^{1,2} and approximately 7% of all men.^{3,4} Teratozoospermia is the leading clinical manifestation of male sterility, and is characterized by sperm head defects accompanied by sperm DNA damage.⁵ Teratozoospermia may affect the outcomes of assisted reproductive techniques,⁶ and is caused by mutations in several genes, including *AURKC*, *SPATA16*, *DPY19L2*, *DNAH1* and *SEPT12*.^{7–9}

In the past decade, the identification of genetic variations (e.g., copy number variation, deletion, insertion, and nucleotide alterations) associated with male infertility using next-generation sequencing (NGS) has increased.⁸ However, research on the aetiology of male infertility typically focuses on specific patient subgroups, such as men with teratozoospermia. NGS has been used to examine various subtypes of teratozoospermia, such as sperms with multiple flagellar morphological abnormalities,¹⁰ cases of primary ciliary dyskinesia-associated male infertility,¹¹ and globozoospermia.¹² However, many plausible causes of male infertility have yet to be replicated and the aetiology may vary between populations.⁸

AGTPBP1 is predominantly expressed in the testes and brain,¹³ and comprises an armadillo-type fold and a carboxypeptidase A domain.¹³ The enzymatic functions of the carboxypeptidase A domain specifically remove polyglutamate from the C-terminus of α -tubulin and generate Δ -2 tubulin.^{14–16} Conversely, tubulin tyrosine ligase-like family proteins (TTL) add polyglutamate.^{17,18} *AGTPBP1* mutations can cause childhood-onset neurodegeneration with cerebellar atrophy (CONDCA) by decreasing deglutamylase activity and the protein amount of Δ -2 tubulin.¹⁹ Furthermore, deletion of the *Agtpbp1* allele in spontaneous strain mice not only causes neuronal degeneration but also results in male infertility.^{20,21} *AGTPBP1* regulates the post-translational modifications of tubulin, such as polyglutamation, and generates Δ -2 tubulin. The development of male germ cells is highly reliant on the dynamics of microtubule structures, such as sperm head shaping and tail formation.^{22,23} We suggest that mutated *AGTPBP1* may be involved in human teratozoospermia.

In this study, we screened patients with teratozoospermia in Taiwan for genetic alterations using whole-exon sequencing (WES)

and identified three genetic mutations in *AGTPBP1*. Notably, the sperm head and tail phenotypes observed in *Agtpbp1*-defective mice resembled those observed in patients carrying *AGTPBP1* missense mutations, providing strong evidence that *AGTPBP1* is a human male infertility gene.

2 | MATERIALS AND METHODS

2.1 | Case enrolment

This study was approved by the Ethics Committee of Cathay General Hospital (IRB approval no: CGH-P102031; CGHFJU-105006). Informed consent was obtained from all recruited patients. Semen samples were obtained by masturbation after 3–5 days of sexual abstinence. After liquefying the semen, routine semen analysis was performed according to the WHO 2010 criteria.²⁴ The results for the selected cases are listed in Table S1. Sperm morphology was evaluated using Kruger's criteria.

2.2 | Genomic DNA extraction, WES and bioinformatic analysis

Genomic DNA was extracted from sperm using a QIAamp DNA Micro Kit according to the manufacturer's instructions and stored at -80°C until the experiment. DNA libraries were prepared using the Illumina TruSeq Exome Library Prep Kit and sequenced using the Illumina NextSeq platform. The average coverage depth was approximately 50x. Sequenced reads were mapped using the Burrows–Wheeler Aligner. WES reads were aligned to the human reference genome (Genome Reference Consortium Human Build 37). Small-copy number variants, insertions, deletions, and variants were identified in individual cases. In collaboration with Professor Donald F. Conrad, the WES outputs were filtered and prioritized using the population sampling probability (PSAP) test, a statistical framework for assessing the significance of variants from single cases of rare genetic diseases.²⁵ The WES data were filtered according to the following rules: (1) read depth > 10, (2) percentage of alternated sites of the reads/all reads > 20%, and (3) PSAP < 0.001. The selected variants were annotated using data from the Exome Aggregation Consortium (ExAC) genome database, and pathogenic effects were predicted using SIFT and PolyPhen-2 softwares. Finally, the mutated sites of the candidate

genes were confirmed by Sanger sequencing after polymerase chain reaction (PCR) using the reference transcript of *AGTPBP1* (NM_001286717.1). The following primes were used for the genomic typing of *AGTPBP1*: forward (F': GGCTTCTGAGGGTT AATGG AG) and reverse (R': TGGGGCTGAAGTAGGGTCTAA). To determine the effects of mutations within the protein structure, three-dimensional (3D) models of mutated-*AGTPBP1* were predicted using ColabFold²⁶ and the carboxypeptidase domain as templates. The results were visualized using PyMOL software (PyMol Molecular Graphics System, Version 2.5.4).

2.3 | Immunofluorescence assay (IFA) and transmission electron microscopy (TEM)

The *AGTPBP1* localization profile in human testicular sections was obtained from The Human Protein Atlas (<https://www.proteinatlas.org/ENSG00000135049-AGTPBP1/tissue/testis#img>).²⁷ For IFA, slides were treated with 0.1% Triton X-100, washed twice with Tris-buffered saline (TBS), and incubated with the primary antibody (rabbit anti-*AGTPBP1* antibody, 1:1000 dilution, Proteintech, Cat. No.14067-1-AP; rabbit anti- δ -2 tubulin antibody, 1:500 dilution, Millipore, Cat. No.AB3203; mouse anti-polyglutamylation modification antibody, 1:2000 dilution, AdipoGen, Cat. No.AG-20B-0020) at room temperature for 60 min. After washing with TBS, the sections were incubated with secondary antibody for 60 min at room temperature and washed again with TBS. An acrosome (lectin PNA, Thermo Fisher Scientific, Cat. No.L32458) and mitochondrial markers (Mito-Tracker Red, Thermo Fisher, Cat. No.M7512) were used for the orientation. For TEM, spermatozoa were washed in 0.1 M phosphate buffer (pH 7.2), fixed and processed according to the protocol described in our previous study.²⁸ The final sections were counterstained with lead citrate and uranyl acetate and observed using a JOEL 1200 TEM.²⁹

2.4 | Preparation of the murine testicular germ cell populations

All animal studies were approved by the Institutional Animal Care and Use Committee (No: A10871, date of approval: 04/10/2020; No: A10979, date of approval: 03/18/2021) of Fu Jen Catholic University. Murine male germ cells were isolated using a centrifugal system according to the density of different types of germ cells, as described previously.²⁸ Briefly, testes were decapsulated and the seminiferous tubules were enzymatically digested, after which the germ cell suspensions were filtered through 35- μ m nylon filters (Falcon). The suspension of single cells was centrifuged at different gravity levels on a Kubota centrifuge 3330. Germ cells were collected at different developmental stages. Mature spermatozoa were collected from the cauda epididymides of adult male mice.

Finally, suspended male germ cells were spread on a slide and air-dried for further analysis.

2.5 | Generation of *Agtbbp1* knockout mice using CRISPR/Cas9

sgRNA was designed by the Gene Knockout Mouse Core Laboratory of the National Taiwan University Center of Genomic Medicine to delete the critical functional carboxypeptidase domain of the *Agtbbp1* allele. The generated sgRNAs and Cas9 targeted the genomic *Agtbbp1* allele in C57BL/6 mouse embryonic stem cells (MESEs) to create a deletion (del) region (Figure 4A). After replacing the wild-type allele in MESEs, clones bearing the targeted allele were confirmed using PCR and sequencing. The confirmed clones were injected into C57BL/6J blastocysts. Blastocysts were transferred to pseudopregnant female mice. Male chimeras were mated with wild-type females to generate *Agtbbp1*^{+/-del} mice. The reproductive ability of each group was compared among pups from the same pregnancy.

2.6 | Sperm quality analysis

Spermatozoa collected from enrolled patients or the vas deferens of wild-type ($n=5$), *Agtbbp1*^{+/-del} ($n=5$), and *Agtbbp1*^{del/del} ($n=6$) adult male mice was suspended in human tubal fluid (HTF) medium (Irvine Scientific). To determine sperm counts, sperm were immobilized by dilution in water and counted using a haemocytometer in duplicate. To evaluate sperm morphology, the sperm medium was diluted to 10⁶/mL with HTF and spotted onto a glass slide. A total of 200 sperms (both motile and immotile) were counted under a microscope in duplicate to obtain the average percentage of motility.

2.7 | Immunoblotting

Testicular tissues and sperms were homogenized using a tissue homogenizer in lysis buffer (20 mM Tris/HCl [pH 8], 150 mM NaCl, 5 mM MgCl₂, 0.5% Triton-X 100, 10% glycerol and a protease inhibitor cocktail). Total lysates were incubated for 30 min on ice and centrifuged at 10,000 \times g and 4°C for 20 min. Protein extracts were heated for 5 min at 37°C before sodium dodecyl sulfate-polyacrylamide gel electrophoresis was performed on an 8% gel.³⁰ The separated proteins were transferred onto polyvinylidene fluoride membranes and incubated with antibodies (rabbit anti-*AGTPBP1*, Proteintech, Cat No. 14067-1-AP; rabbit anti- δ -2 tubulin, Millipore, Cat. No.AB3203; mouse anti-polyglutamylation modification tubulin, AdipoGen, Cat. No.AG-20B-0020; mouse anti-GAPDH antibody, Sigma-Aldrich, Cat. No. G8795) and detected using a chemiluminescence detection system.

3 | RESULTS

3.1 | Identification of the novel genetic alterations in patients with teratozoospermia

To explore the genetic causes of teratozoospermia in Taiwan, we enrolled 254 males with infertility, defined as those with one or more abnormal semen parameters. Twelve patients with severe morphological sperm defects were selected (Table S1) and WES was performed. The identified genetic variants were evaluated using the PSAP test, allele frequencies from ExAC, and the pathogenicity predictors PolyPhen and SIFT (Figure 1A). Finally, heterozygous variants in seven teratozoospermia-related genes were predicted to be potentially deleterious (Figure 1A: *PLK4*: p.Pro953Leu; *AGTPBP1*: p.Glu423Asp, p.Pro653Leu, p.Arg811His; *GRID2*: p.Arg631Gln; *KISS1R*: p.Pro196His; *P2RX2*: p.Ala182Ser; *MEIG1*: p.Asp63Asn; *PIWIL2*: p.Thr937Ser). One of the candidate genes, *AGTPBP1*, is remarkable, as a classical spontaneous *Agtbbp1* mouse mutant has been shown to exhibit abnormal sperm development in previous studies.^{20,21} Genetic changes in *AGTPBP1* were observed in both cases. Affected individual A carried compound heterozygous mutations (NM_001286717.1: c.1336A>T [p.Glu423Asp] and c.1959C>T [p.Pro653Leu]) (Figure 1B). The other hemizygous mutation (NM_001286717.1: c.2499G>A [p.Arg811His]) was detected in affected individual B. (Figure 1C). Both PolyPhen and SIFT predicted that two amino acid changes (p.Pro653Leu and p.Arg811His) damaged the protein (Figure 1A). Furthermore, the changed site of p.Arg811His localized within the critical carboxypeptidase A domain of *AGTPBP1* (Figures 1C,D). The predicted 3D protein structure revealed that the substitution of Arg811 with His would likely disrupt the oxygen-hydrogen bonding between nearby amino acids (p.Gln793, Leu1117, and Ile1130), potentially affecting structural stability and destabilizing the overall functional structure (Figure 1E). In summary, based on WES and bioinformatics tests, several genetic alterations were identified in patients with teratozoospermia, and *AGTPBP1* genetic variations appeared to be associated with human teratozoospermia.

3.2 | Spermatozoa from patients with altered *AGTPBP1* revealed severe morphological defects

Immunostaining and TEM were used to examine genetic changes in *AGTPBP1* in spermatozoa. *AGTPBP1* was expressed in spermatocytes (black arrows) and was strongly expressed in spermatids (red arrows) in human testicular sections obtained from the Human Protein Atlas database (Figure 2A). Immunofluorescence staining of human spermatozoa revealed that *AGTPBP1* was mainly localized in the neck (white arrows) and annulus (red arrows), which are ring-like structures separating the midpiece and principal regions of the tail (Figure 2B; left panel). Spermatozoa from the affected individual A exhibited compound heterozygous mutations of *AGTPBP1* (NM_001286717.1: c.1336A>T [p.Glu423Asp] and c.1959C>T

[p.Pro653Leu]), while affected individual B carried a hemizygous mutation of *AGTPBP1* (c.2499G>A [p.Arg811His]) that resulted in head defects (Figure 2B; middle panel) and lack of tail development (Figure 2B; left panel), respectively. Contrast immunostaining using sperm from the control, affected individual A, and affected individual B revealed mislocalized *AGTPBP1* signals to the midpiece that had fragmented patterns (white arrows). Furthermore, spermatozoa from affected individual B showed significantly decreased *AGTPBP1* signals (Figure 2B; Right panel). TEM revealed severe morphological and size abnormalities of the sperm head of spermatozoa from affected individual B (Figure 2C; red arrows). Most sperm showed no tail development, and a small portion of the sperm with tails showed disarranged mitochondria (Figure 2C; black arrows). These results indicated that genetically altered *AGTPBP1* expression resulted in spermatozoa with severe head and tail defects.

3.3 | Dynamic patterns of *AGTPBP1* during murine spermiogenesis

To determine the precise localization and possible reproductive role of *AGTPBP1* during murine spermiogenesis, testicular germ cell populations were separated and subjected to immunostaining. In steps 1–7, round spermatids containing *AGTPBP1* were distributed around the whole cells (Figure 3A). During shaping of the sperm head in steps 8–10, *AGTPBP1* moved towards the post-acrosomal region and was then recruited to the manchette structure in steps 11–13 (Figure 3B). Subsequently, *AGTPBP1* was concentrated at the sperm neck (Step 14), followed by the removal of the middle piece at steps 15–16 (Figure 3C). In mature caudal epididymal spermatozoa, *AGTPBP1* was localized in the midpiece region (Figure 3C). These results suggest that *AGTPBP1* is highly expressed during spermiogenesis and is likely involved in sperm head and tail formation.

3.4 | Loss of *Agtbbp1* in mice causes severe morphological defects in the sperm

To further test the causal relationship between genetic changes in *AGTPBP1* and male sterility, we generated an *Agtbbp1*^{del} mouse line. (Figure 4A). *AGTPBP1*-deficient mice were confirmed by genotyping and immunoblotting (Figure 4B,C). *Agtbbp1*^{del/del} mice were completely sterile when paired with controls (wild-type male mice: 8±0.82 pups per litter, n=5 vs. *Agtbbp1*^{del/del} male mice: 0 pups per litter, n=6). Sperm isolated from the vas deferens and epididymis of *Agtbbp1*^{del/del} male mice revealed severe abnormalities in sperm morphology and motility (wild-type: n=5; *Agtbbp1*^{+/-del}: n=5; *Agtbbp1*^{del/del}: n=6) (Figure 4 D–G). Notably, sperm morphology in *Agtbbp1* null mice displayed severe defects, such as immature sperm (no tail development) and tail defects (Figure 4D,F), which was similar to the results observed in *AGTPBP1*-mutated patients (Figure 2B,C). These results revealed that *AGTPBP1* is required for normal sperm development and male fertility (Figure 4).

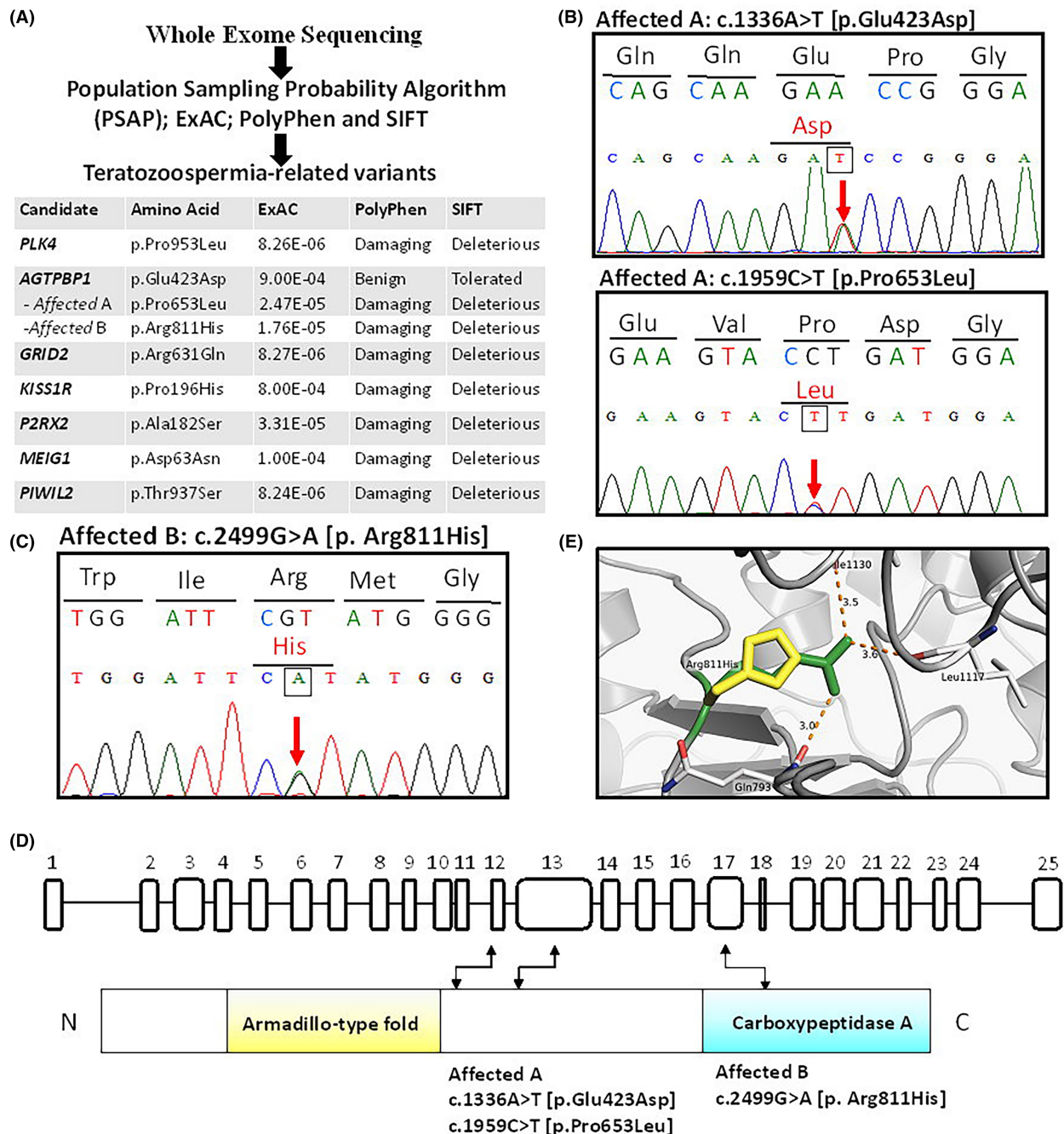


FIGURE 1 Identification of *ATP/GTP Binding Protein 1* (*AGTPBP1*) genetic alterations in teratozoospermia using whole-exome sequencing (WES). (A) Screening for genetic changes in 12 teratozoospermia cases using WES and the results of bioinformatic analysis (PSAP; ExAC; PolyPhen, and SIFT). (B, C) Sanger sequencing chromatograms of *AGTPBP1* variants. Chromatograms display the sequence corresponding to the control and mutated alleles (upper and lower panels, respectively). Genetic changes in *AGTPBP1* in affected individual A carrying compound heterozygous mutations (NM_001286717.1: c.1336A>T [p.Glu423Asp]; c.1959C>T [p.Pro653Leu]) and affected individual B carrying a hemizygous mutation (NM_001286717.1: c.2499G>A [p. Arg811His]). Red arrows indicate the site changes compared with control cases. (D) Schematic of the *AGTPBP1* gene (upper panel) and protein (lower panel). The 25 exons of the human *AGTPBP1* were numbered. N = N-terminal; C = C-terminal. The near N-terminal and C-terminal regions of *AGTPBP1* are encoded with the armadillo-type fold and carboxypeptidase A, respectively. The amino acid of p.Arg811His was located in exon 17 of *AGTPBP1*. (E) The substitution of arginine (green colour) with histidine (yellow colour) (p.Arg811His) in the predicted carboxypeptidase A domain structure disrupts the oxygen-hydrogen bonding between the nearby amino acids (p.Gln793, Leu1117, and Ile1130).

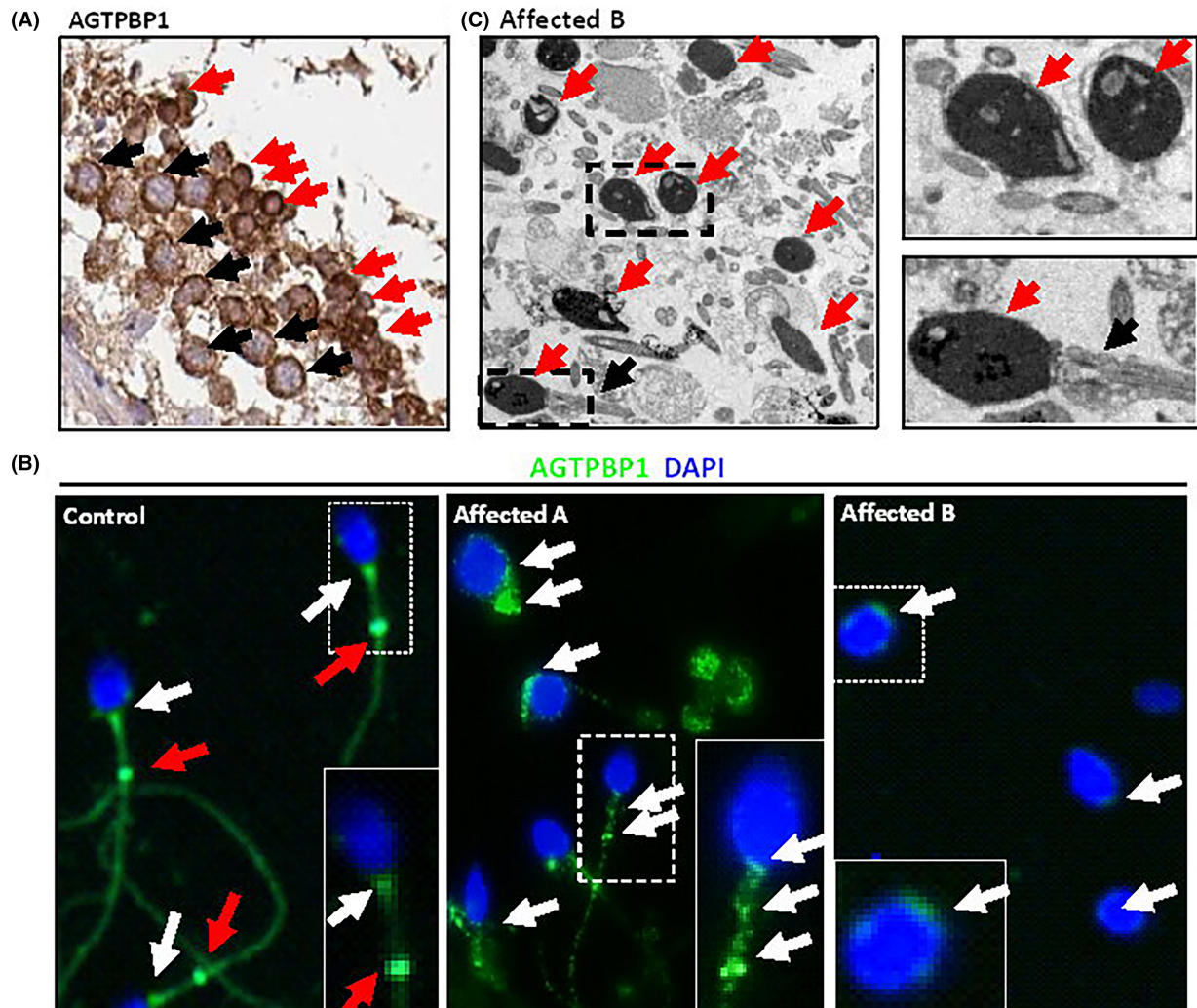


FIGURE 2 Immunostaining and electron microscopy analysis in cases with *ATP/GTP Binding Protein 1* (*AGTPBP1*) mutations. (A) Immunohistochemical detection of *AGTPBP1* signals in the human testicular sections from The HUMAN PROTEIN ATLAS. Black and red arrows indicate the signals on spermatocytes and spermatids, respectively. (B) Sperm from the control (Left), affected individual A carrying compound heterozygous mutations (NM_001286717.1: c.1336A > T [p.Glu423Asp]; c.1959C > T [p.Pro653Leu]), and affected individual B carrying a hemizygous mutation (NM_001286717.1: c.2499G > A [p.Arg811His]). *AGTPBP1* is mainly located at the sperm neck (white arrows) and annulus (red arrows) in control cases. *AGTPBP1* signals (white arrows) denote the disrupted patterns (fragmented) (Middle and Left) and decreased *AGTPBP1* signals (Left). Sperm head stains with nuclear dye (DAPI; blue). The sperm is marked in the dotted rectangle and enlarged in the right corner. (C) Electron microscopy images of sperm from affected individual B showing severely malformed head shapes (red arrow) and sperm tail defects (black arrow). Enlarge figures have shown as the right panels.

3.5 | *Agtppb1* deficiency affects the de-polyglutamylation of tubulin during sperm development

The precise regulation and maintenance of tubulin stability are vital for the morphological formation of the sperm head and elongation of the tail, which are dependent on the stabilization of the microtubule structure.²² Precise regulation of the balance between polyglutamylation (poly-E) and de-polyglutamylation in the C-terminal region of tubulin is mediated by TLL and *AGTPBP1*^{16,31} (Figure 5A). Therefore, we hypothesized that the loss of *AGTPBP1* in mice results in an overabundance of polyglutamylated microtubules in developing germ cells and sperm. To test this hypothesis, we performed

immunoblotting and immunostaining of *Agtppb1*-deficient testicular tissues to evaluate whether the loss of *Agtppb1* affected the stability of poly-E tubulin. Compared to wild-type mice, the testicular tissues of *Agtppb1*-deficient mice showed abnormal poly-E tubulin lengths (Figure 5B). Within germ cells from wild-type mice, poly-E tubulin was organized as a filamentous manchette structure in elongating spermatids and elongated spermatids during sperm head formation (Figure 5C-a,b). Furthermore, poly-E tubulin was present in the tails of mature sperm (Figure 5C-c). In contrast, the loss of *Agtppb1* in mice resulted in disorganized poly-E tubulin in sperm with no tail development (Figure 5D-a,b) or a defective tail (bent and curled) (Figure 5D-c,d). Thus, the loss of *Agtppb1* disrupts the stability of poly-E-tubulin, which is critical for sperm head and tail formation.

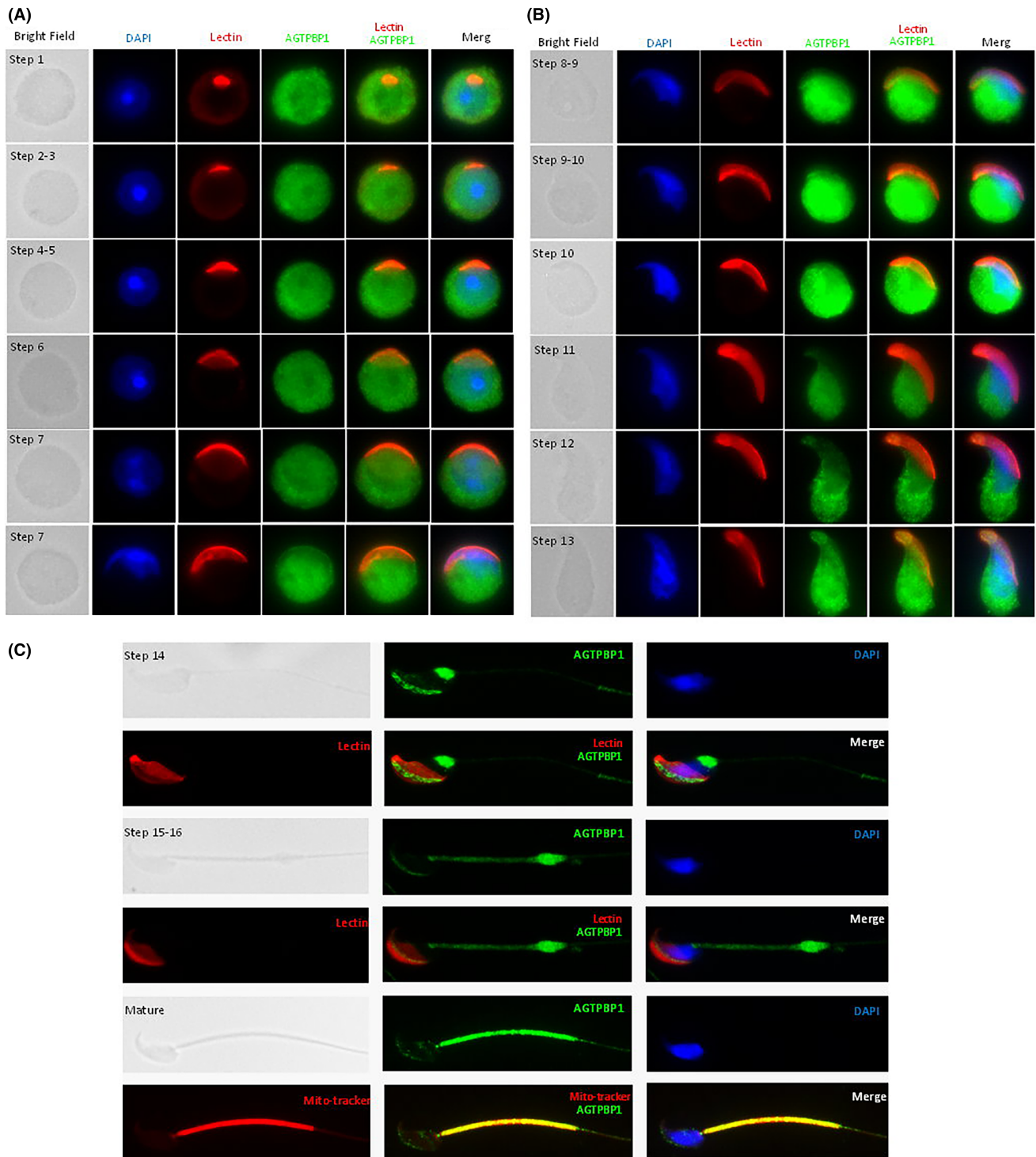


FIGURE 3 ATP/GTP Binding Protein 1 (AGTPBP1) signals showed multiple localizations during murine spermiogenesis. From left to right: bright field, DAPI staining (blue), lectin staining (acrosome marker; red), AGTPBP1 staining (green), AGTPBP1 staining (green) combined with lectin, and AGTPBP1 signals (lectin; AGTPBP1) combined with DAPI (Merge). (A–C) AGTPBP1 signals localized at different steps of murine spermiogenesis: step 1, step 2–3, step 4–5, Step 6, step 7, step 8–9, step 9–10, step 10, step 11, step 12, step 13, step 14, step 15–16, and mature sperm (co-staining with Mito-tracker). 400X magnification.

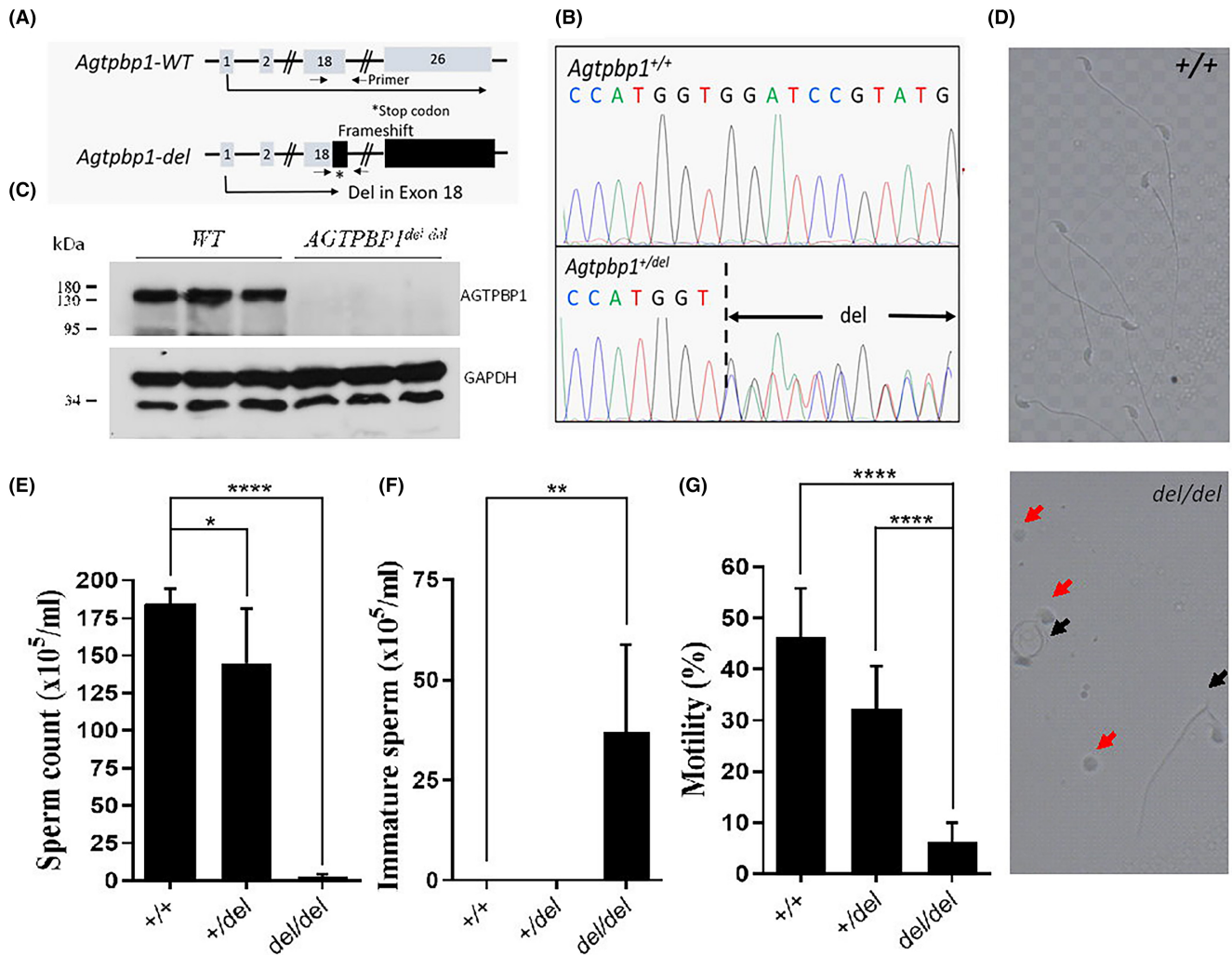


FIGURE 4 Disruption of ATP/GTP Binding Protein 1 (*Agtbbp1*) allele in mice results in male sterility. (A) Schematic representation of the murine genomic structure and disrupted exon 18 of *Agtbbp1* induces frameshift mutation. (B) Sanger sequencing reveals the specific deletion (del) sites within exon 18 in *Agtbbp1*^{+/} mice, compared with wild-type mice. (C) AGTPBP1 expression was evaluated in the murine testes of *Agtbbp1*^{del/del} mice via western blotting. (D) Sperm collected from vas deferens of *Agtbbp1*^{del/del} mice shows immature sperm (round-like; red arrows) and defective sperm tail (black arrows), compared with the wild-type mice (upper). (E–G.) Analysis of the ratio of sperm count, immature sperm (round-like), and motility in 2-month-old wild-type and *Agtbbp1*^{del/del} mice. Mice number per genotype: wild-type, $n=5$; *Agtbbp1*^{+/}, $n=5$; *Agtbbp1*^{del/del}, $n=6$. Sperm number > 200 per mouse. Each bar represents the mean \pm standard error of the mean (SEM). *Significant differences (* $p < 0.05$; ** $p < 0.001$; **** $p < 0.00001$, analysed using Student's t test).

3.6 | Loss of AGTPBP1 decreases the amount and disturbs the localization of Δ -2 tubulin during sperm head and tail formation

The deglutamylation activity of AGTPBP1 is a critical step for Δ -2 tubulin generation (Figure 6A). Therefore, we investigated whether the disrupted *Agtbbp1* allele affected the generation of Δ -2 tubulin. Figure 6B shows a significant decrease in the amount of Δ -2 tubulin in the *Agtbbp1*^{del/del} testis, compared with that in wild-type mice. In wild-type mice, Δ -2 tubulin is a major component of the manchette (Figure 6C-a,b) and sperm tail (Figure 6C-c) at various developmental stages: elongating spermatids, elongated spermatids, and mature sperm. In contrast, the loss of AGTPBP1 function resulted in a disrupted Δ -2 tubulin structure within the sperm with no tail

development (Figure 6D-a,b) and morphologically defective sperm (Figure 6D-c,d). Collectively, these data indicate that AGTPBP1 plays an essential role in the generation of Δ -2 tubulin in developing male germ cells (Figure 6).

4 | DISCUSSION

In this study, three sporadic genetic alterations in *AGTPBP1* in Taiwanese patients with teratozoospermia were identified using WES. Sperm from affected patients showed severe structural head and tail defects. AGTPBP1 was mainly observed during murine sperm head formation and tail elongation during spermiogenesis. Consistent with these findings, sperm from a *Agtbbp1* deletion

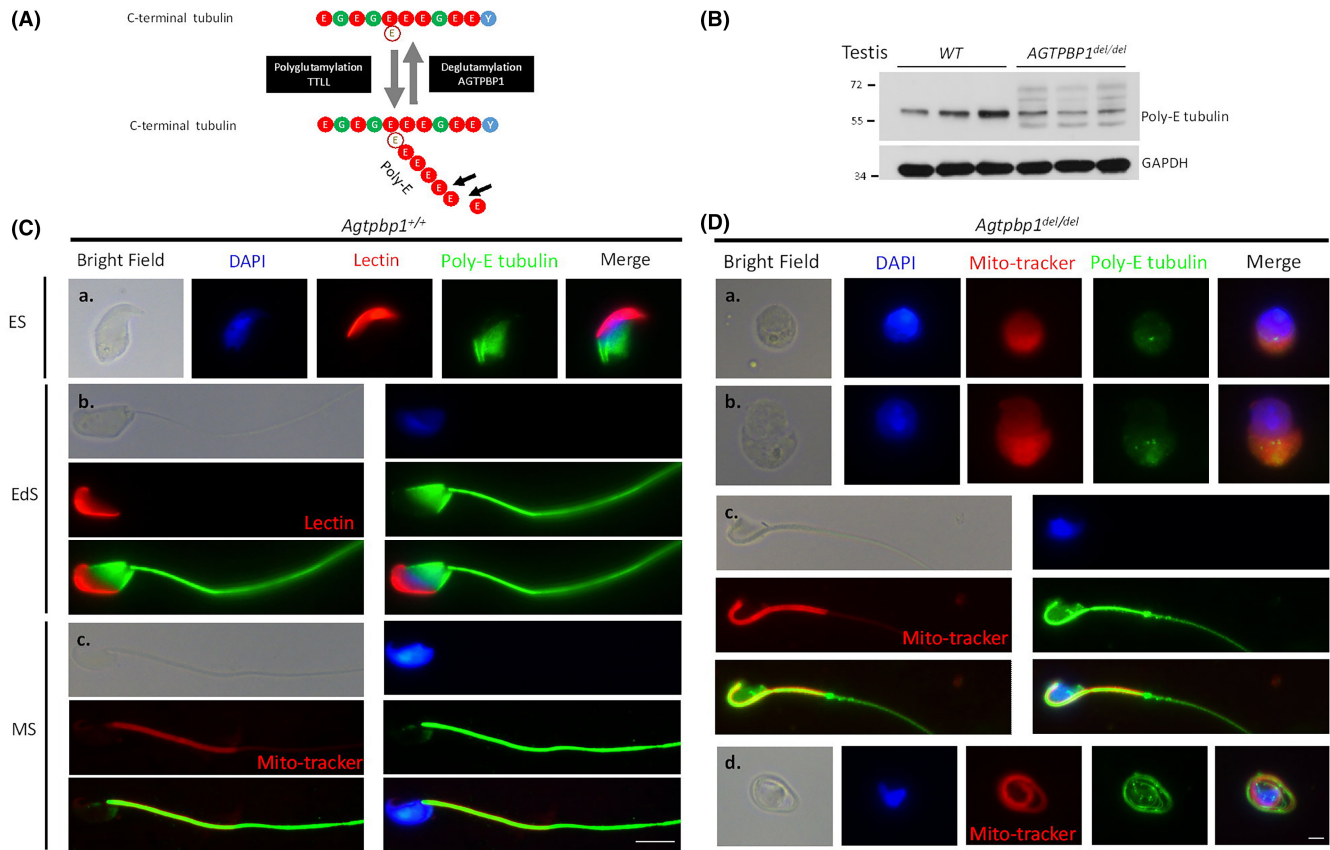


FIGURE 5 Loss of ATP/GTP Binding Protein 1 (AGTPBP1) affects its enzymatic function of depolyglutamation. (A) Diagrammatic representation of the tubulin tyrosine ligase-like family protein (TLL) and AGTPBP1 catalysing the polyglutamylation and depolyglutamation of C-terminal amino acids of tubulin, respectively. E: Glutamine; G: Glycine; Y: Tyrosine; poly-E: Poly-glutamylation. (B) Amounts of polyglutamylated tubulin of various sizes were determined in the murine testicular tissue of *Agtppb1^{del/del}* mice ($n=3$) via immunoblotting, compared with wild-type ($n=3$). (C) Different developmental steps of male germ cells and mature sperm isolated from wild-type murine testis and vas deferens, respectively. (a) Elongating spermatids (ES); (b) elongated spermatids (EdS); and (c, d) mature sperm (MS). (D) Sperm isolated from vas deferens of *Agtppb1^{del/del}* mice. (C, D) From left to right: bright field, DAPI staining (blue), lectin staining (acrosome marker; red), anti-polyglutamylated tubulin (poly-E tubulin; green), and combined with DAPI, lectin, and poly-E tubulin signals (Merge). Mature sperm co-stained with Mito-tracker (midpiece marker) (400X magnification).

mouse model exhibited morphological defects in the head and tail. At the molecular level, the loss of *Agtppb1* resulted in an abnormal poly-E tubulin length and decreased $\Delta-2$ tubulin generation in vivo. To the best of our knowledge, this is the first study to link genetic changes in *AGTPBP1* with teratozoospermia from a clinical perspective.

4.1 | Identification of male sterility-related genetic changes in Taiwan from WES

Several studies investigating sterility-related genetic alterations have been conducted; however, these genetic alterations differ among populations. In this study, deleterious genetic changes were identified in seven genes using WES and data obtained from PSAP, ExAC, PolyPhen, and SIFT analyses. Five of these genes were characterized as male infertility-related genes, including *Polo-like kinase*

4 (*PLK4*), *AGTPBP1*, *KISS1 receptor*, *Meiosis Expressed Gene 1 (MEIG1)*, and *Piwi Like RNA-Mediated Gene Silencing 2 (PIWIL2)* (Figure 1). *PLK4*, which belongs to the polo protein family of serine/threonine protein kinases,^{32,33} is located in centrioles, which are microtubule-based structures within centrosomes, and is involved in centriole formation.³³ In clinical observations, a heterozygous 13-bp deletion in the serine/threonine kinase domain of *PLK4* was identified in azoospermia cases with Sertoli cell-only syndrome (SCOS),³⁴ and a heterozygous *PLK4* mutation (p.Ile242Asn) in mice caused male germ cell loss in the testes,³⁵ similar to that in human SCOS. Another gene, *MEIG1*, is involved in meiosis.³⁶ *Meig1* knockout in male mice results in sterility because of the arrest of spermiogenesis before the completion of spermatid elongation.³⁷ TEM revealed that the manchette structure was disrupted in spermatids of *Meig1*-deficient mice. Based on previous reports, the mutated genes identified using WES in this study appear to be potential causative candidates for male infertility in Taiwan.

and thalamic neurons.^{40,41} In addition to neuronal degeneration, *pcd* mutant male mice also exhibit male sterility, with decreased sperm counts and few mature sperm.³² After genetic mapping, the mutated gene of the *pcd* strain mice was mapped to chromosome 13, and mutations, deletions, and insertions of genomic fragments within the *AGTPBP1* gene were identified in *pcd*^{2j}, *pcd*^{3j}, and *pcd*^{5j} strains,^{20,42} respectively. The mRNA expression levels of *AGTPBP1* were found to be reduced in the brain and testis tissues of *pcd* mice.^{20,42} Kim et al. (2011) first detected *AGTPBP1* in spermatozoa and found it to be primarily expressed in round spermatids in testicular sections.²¹ Loss of the *AGTPBP1* allele in *pcd*^{3j} mice decreased testicular weight, increased apoptotic cell death in the testes, and produced abnormally shaped spermatozoa from the cauda epididymis.³⁷ However, the detailed dynamic expression patterns and in vivo functions of *AGTPBP1* during sperm morphological development remain unclear. In this study, we found that *AGTPBP1* was specifically localized around the manchette structure of the sperm head and elongating tail during murine spermiogenesis (Figure 3). Significantly reduced sperm count and motility and an increased number of immature (no tail development) and tail-defective sperm were observed in our *Agtpbp1*-knockout mice (Figure 4). Immature sperm are released from the seminiferous tubules owing to disrupted sperm development. These findings indicate that *AGTPBP1* is critical for sperm head and tail formation during murine spermatogenesis.

4.4 | Deglutamylation activity of AGTPBP1 is critical for the formation of sperm head and tail in mice

The balance between polyglutamylation and deglutamylation in the C-terminus of tubulin is critical for the stability of the microtubule structure during neuronal development.⁴³ Polyglutamylases and

deglutamylation modifications are catalysed by tubulin tyrosine ligase-like proteins, TTLL family proteins, and cytosolic carboxypeptidase family proteins (e.g., *AGTPBP1*).^{44,45} Using *pcd* strain, Shashe et al. reported that the femoral quadriceps nerve of *pcd*^{3j} mice exhibited a reduction in nerve diameter and the number of myelinated axons formed via microtubule polymerization.¹⁹ Furthermore, the cerebellum of *pcd*^{3j} mice exhibited the increased tubulin polyglutamylation and decreased Δ -2 tubulin generation. These results support the hypothesis that *AGTPBP1* is critical for maintaining microtubule structure, the major cytoskeletal component of the axon, and preserves neuron numbers. In this study, *Agtpbp1* ablation in mice revealed similar results: an increase in abnormally sized polyglutamylated tubulin and decrease in Δ -2 tubulin levels (Figure 5B and 6B). Compared with signals from wild-type mice, the multiplex sizes of polyglutamylated tubulin and Δ -2 tubulin exhibited fragmented patterns during sperm head and tail formation (Figure 5C and 6C). Therefore, we suggest that the deglutamylation activity of *AGTPBP1* is critical for the formation and maintenance of neurons and male germ cells.

4.5 | Enzymatic and molecular roles of AGTPBP1 during murine spermiogenesis

Based on our results and those of previous studies, we proposed a possible molecular model of *AGTPBP1* during spermiogenesis (Figure 7). *AGTPBP1* was highly localized in the manchette structure in the heads of elongating spermatids and the tails of mature sperm (Figure 3). The manchette, a temporary microtubule and an actin-based structure, facilitates the transport of vesicles and proteins necessary for the formation of the sperm head and tail.^{22,46} Figure 7A shows that polyglutamylation and depolyglutamylation of the C-terminal sequences of tubulin are catalysed by TTLL and *AGTPBP1*, respectively, to balance long-chain polyglutamylation

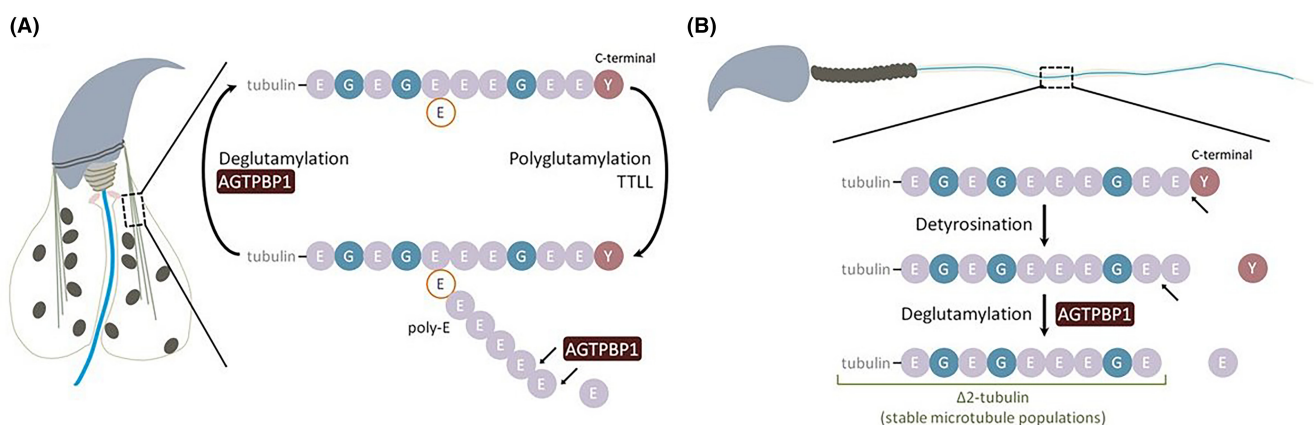


FIGURE 7 Possible enzymatic and molecular roles of ATP/GTP Binding Protein 1 (*AGTPBP1*) in sperm head and tail formation. During the elongation of the sperm head and tail, *AGTPBP1* is highly localized at the manchette (A) and axoneme (B). (A) The polyglutamylation and depolyglutamylation of C-terminal sequences of tubulin were catalysed by tubulin tyrosine ligase-like family proteins (TTLL) and *AGTPBP1*, respectively, to balance the long chain of polyglutamylation in tubulin. (B) *AGTPBP1* also catalyses the generation of Δ -2-tubulin (stable microtubules), which requires prior detyrosination. E, glutamine; G, glycine; Y, tyrosine; poly-E, poly-glutamylation.

in tubulin. AGTPBP1 also catalyses the generation of Δ 2-tubulin to form stable microtubulin after the detirosination of tubulin (Figure 7B). In AGTPBP1-defective mice, the manchette and sperm tail structures were disrupted (Figures 5 and 6) due to the impairment of the enzymatic functions of AGTPBP1.

The present study is the first to establish a connection between the genetic mutations in AGTPBP1 to teratozoospermia. Damage to AGTPBP1 in human and mouse sperm results in severe sperm tail and head defects, leading to the loss of deglutamylation function. This study identifies the role of AGTPBP1 mutations in teratozoospermia and provides potential guidance for the diagnosis and treatment of male infertility.

AUTHOR CONTRIBUTIONS

Yu-Hua Lin: Conceptualization (equal); data curation (equal); funding acquisition (equal). **Ya-Yun Wang:** Data curation (equal); investigation (equal); project administration (equal). **Tsung-Hsuan Lai:** Data curation (equal); methodology (equal); resources (equal). **Jih-Lung Teng:** Investigation (equal); methodology (equal); software (equal). **Chi-Wei Lin:** Investigation (equal); software (equal). **Chih-Chun Ke:** Funding acquisition (equal); investigation (equal). **I-Shing Yu:** Investigation (equal); methodology (equal). **Hui-Ling Lee:** Investigation (equal); methodology (equal). **Chying-Chyuan Chan:** Investigation (equal); resources (equal). **Chi-Hua Tung:** Software (equal); visualization (equal). **Donald F. Conrad:** Formal analysis (equal); methodology (equal); software (equal). **Moira K. O'Bryan:** Conceptualization (equal); writing – original draft (equal); writing – review and editing (equal). **Ying-Hung Lin:** Conceptualization (equal); funding acquisition (lead); writing – original draft (equal).

ACKNOWLEDGEMENTS

This study was supported by grants from the National Science and Technology Council in Taiwan (NSTC 111-2320-B-030 -007-MY3), Ministry of Science and Technology of the Republic of China (MOST 109-2320-B-030-002-; MOST 110-2320-B-030-002-), and Cardinal Tien Hospital (CTH-112A-2209). We thank the technical services provided by the "Transgenic Mouse Model Core Facility of the National Core Facility for Biopharmaceuticals, National Science and Technology Council, Taiwan," and the "Animal Resources Laboratory of the National Taiwan University Center of Genomic and Precision Medicine." We also thank Mr. Yen-sheng Wu for technical assistance provided by the Electron Microscope Laboratory of Tzong Jwo Jang at the College of Medicine, Fu Jen Catholic University.

CONFLICT OF INTEREST STATEMENT

The authors declare that they have no conflicts of interest.

DATA AVAILABILITY STATEMENT

The data that support the findings of this study are available on request from the corresponding author. The data are not publicly available due to privacy or ethical restrictions.

ORCID

Chi-Hua Tung  <https://orcid.org/0000-0002-7232-312X>

Ying-Hung Lin  <https://orcid.org/0000-0002-1574-1579>

REFERENCES

- Vayena ERP, Griffin PD. *Current Practices & Controversies in Assisted Reproduction: Report of a WHO Meeting*. Switzerland WHO; 2001.
- Boivin J, Bunting L, Collins JA, Nygren KG. International estimates of infertility prevalence and treatment-seeking: potential need and demand for infertility medical care. *Hum Reprod*. 2007;22(6):1506-1512. doi:10.1093/humrep/dem046
- Agarwal A, Baskaran S, Parekh N, et al. Male infertility. *Lancet*. 2021;397(10271):319-333. doi:10.1016/S0140-6736
- Krausz C, Riera-Escamilla A. Genetics of male infertility. *Nat Rev Urol*. 2018;15(6):369-384. doi:10.1038/s41585-018-0003-3
- Ammar O, Mehdi M, Muratori M. Teratozoospermia: its association with sperm DNA defects, apoptotic alterations, and oxidative stress. *Andrology*. 2020;8(5):1095-1106. doi:10.1111/andr.12778
- Shabtaie SA, Gerkowicz SA, Kohn TP, Ramasamy R. Role of abnormal sperm morphology in predicting pregnancy outcomes. *Curr Urol rep*. 2016;17(9):67:67. doi:10.1007/s11934-016-0623-1
- Coutton C, Escoffier J, Martinez G, Arnoult C, Ray PF. Teratozoospermia: spotlight on the main genetic actors in the human. *Hum Reprod Update*. 2015;21(4):455-485. doi:10.1093/humupd/dmv020
- Houston BJ, Riera-Escamilla A, Wyrwoll MJ, et al. A systematic review of the validated monogenic causes of human male infertility: 2020 update and a discussion of emerging gene-disease relationships. *Hum Reprod Update*. 2021;28(1):15-29. doi:10.1093/humupd/dmab030
- Wang YY, Lai TH, Chen MF, Lee HL, Kuo PL, Lin YH. SEPT14 mutations and Teratozoospermia: genetic effects on sperm head morphology and DNA integrity. *J Clin Med*. 2019;8(9):1297. doi:10.3390/jcm8091297
- Amiri-Yekta A, Coutton C, Kherraf ZE, et al. Whole-exome sequencing of familial cases of multiple morphological abnormalities of the sperm flagella (MMAF) reveals new DNAH1 mutations. *Hum Reprod*. 2016;31(12):2872-2880. doi:10.1093/humrep/dew262
- Moore DJ, Onoufriadis A, Shoemark A, et al. Mutations in ZMYND10, a gene essential for proper axonemal assembly of inner and outer dynein arms in humans and flies, cause primary ciliary dyskinesia. *Am J Hum Genet*. 2013;93(2):346-356. doi:10.1016/j.ajhg.2013.07.009
- Oud MS, Okutman O, Hendricks LAJ, et al. Exome sequencing reveals novel causes as well as new candidate genes for human globozoospermia. *Hum Reprod*. 2020;35(1):240-252. doi:10.1093/humrep/dez246
- Harris A, Morgan JI, Pecot M, Soumare A, Osborne A, Soares HD. Regenerating motor neurons express Nna1, a novel ATP/GTP-binding protein related to zinc carboxypeptidases. *Mol Cell Neurosci*. 2000;16(5):578-596. doi:10.1006/mcne.2000.0900
- Wu HY, Rong Y, Correia K, Min J, Morgan JI. Comparison of the enzymatic and functional properties of three cytosolic carboxypeptidase family members. *J Biol Chem*. 2015;290(2):1222-1232. doi:10.1074/jbc.M114.604850
- Kuo YC, Shen YR, Chen HI, et al. SEPT12 orchestrates the formation of mammalian sperm annulus by organizing core octameric complexes with other SEPT proteins. *J Cell Sci*. 2015;128(5):923-934. doi:10.1242/jcs.158998
- Rogowski K, van Dijk J, Magiera MM, et al. A family of protein-deglutamylation enzymes associated with neurodegeneration. *Cell*. 2010;143(4):564-578. doi:10.1016/j.cell.2010.10.014

17. Bosch Grau M, Gonzalez Curto G, Rocha C, et al. Tubulin glycosylases and glutamylases have distinct functions in stabilization and motility of ependymal cilia. *J Cell Biol.* 2013;202(3):441-451. doi:[10.1083/jcb.201305041](https://doi.org/10.1083/jcb.201305041)
18. Mahalingan KK, Keith Keenan E, Strickland M, et al. Structural basis for polyglutamate chain initiation and elongation by TTL family enzymes. *Nat Struct Mol Biol.* 2020;27(9):802-813. doi:[10.1038/s41594-020-0462-0](https://doi.org/10.1038/s41594-020-0462-0)
19. Shashi V, Magiera MM, Klein D, et al. Loss of tubulin deglutamylase CCP1 causes infantile-onset neurodegeneration. *EMBO J.* 2018;37(23):e100540. doi:[10.15252/embj.2018100540](https://doi.org/10.15252/embj.2018100540)
20. Fernandez-Gonzalez A, La Spada AR, Treadaway J, et al. Purkinje cell degeneration (pcd) phenotypes caused by mutations in the axotomy-induced gene, Nna1. *Science.* 2002;295(5561):1904-1906. doi:[10.1126/science.1068912](https://doi.org/10.1126/science.1068912)
21. Kim N, Xiao R, Choi H, et al. Abnormal sperm development in pcd(3J)-/- mice: the importance of Agtbbp1 in spermatogenesis. *Mol Cells.* 2011;31(1):39-48. doi:[10.1007/s10059-011-0002-1](https://doi.org/10.1007/s10059-011-0002-1)
22. Dunleavy JEM, O'Bryan MK, Stanton PG, O'Donnell L. The cytoskeleton in spermatogenesis. *Reproduction.* 2019;157(2):R53-R72. doi:[10.1530/REP-18-0457](https://doi.org/10.1530/REP-18-0457)
23. Tang EI, Mruk DD, Cheng CY. Regulation of microtubule (MT)-based cytoskeleton in the seminiferous epithelium during spermatogenesis. *Semin Cell Dev Biol.* 2016;59:35-45. doi:[10.1016/j.semcdb.2016.01.004](https://doi.org/10.1016/j.semcdb.2016.01.004)
24. World Health Organisation. WHO Laboratory Manual for the Examination and Processing of Human Semen, 5th ed. World Health Organization; 2010.
25. Wilfert AB, Chao KR, Kaushal M, et al. Genome-wide significance testing of variation from single case exomes. *Nat Genet.* 2016;48(12):1455-1461. doi:[10.1038/ng.3697](https://doi.org/10.1038/ng.3697)
26. Mirdita M, Schutze K, Moriwaki Y, Heo L, Ovchinnikov S, Steinegger M. ColabFold: making protein folding accessible to all. *Nat Methods.* 2022;19(6):679-682. doi:[10.1038/s41592-022-01488-1](https://doi.org/10.1038/s41592-022-01488-1)
27. Uhlen M, Fagerberg L, Hallstrom BM, et al. Proteomics. Tissue-based map of the human proteome. *Science.* 2015;347(6220):1260419. doi:[10.1126/science.1260419](https://doi.org/10.1126/science.1260419)
28. Lin YH, Lin YM, Wang YY, et al. The expression level of septin12 is critical for spermiogenesis. *Am J Pathol.* 2009;174(5):1857-1868. doi:[10.2353/ajpath.2009.080955](https://doi.org/10.2353/ajpath.2009.080955)
29. Lee JD, Allen MJ, Balhorn R. Atomic force microscope analysis of chromatin volumes in human sperm with head-shape abnormalities. *Biol Reprod.* 1997;56(1):42-49.
30. Grove DE, Rosser MF, Watkins RL, Cyr DM. Analysis of CFTR folding and degradation in transiently transfected cells. *Methods Mol Biol.* 2011;741:219-232. doi:[10.1007/978-1-61779-117-8_15](https://doi.org/10.1007/978-1-61779-117-8_15)
31. Berezniuk I, Vu HT, Lyons PJ, et al. Cytosolic carboxypeptidase 1 is involved in processing alpha- and beta-tubulin. *J Biol Chem.* 2012;287(9):6503-6517. doi:[10.1074/jbc.M111.309138](https://doi.org/10.1074/jbc.M111.309138)
32. Karakaya M, Paketci C, Altmueller J, et al. Biallelic variant in AGTPBP1 causes infantile lower motor neuron degeneration and cerebellar atrophy. *Am J Med Genet A.* 2019;179(8):1580-1584. doi:[10.1002/ajmg.a.61198](https://doi.org/10.1002/ajmg.a.61198)
33. Habedanck R, Stierhof YD, Wilkinson CJ, Nigg EA. The polo kinase Plk4 functions in centriole duplication. *Nat Cell Biol.* 2005;7(11):1140-1146. doi:[10.1038/ncb1320](https://doi.org/10.1038/ncb1320)
34. Miyamoto T, Bando Y, Koh E, et al. A PLK4 mutation causing azoospermia in a man with Sertoli cell-only syndrome. *Andrology.* 2016;4(1):75-81. doi:[10.1111/andr.12113](https://doi.org/10.1111/andr.12113)
35. Harris RM, Weiss J, Jameson JL. Male hypogonadism and germ cell loss caused by a mutation in polo-like kinase 4. *Endocrinology.* 2011;152(10):3975-3985. doi:[10.1210/en.2011-1106](https://doi.org/10.1210/en.2011-1106)
36. Don J, Wolgemuth DJ. Identification and characterization of the regulated pattern of expression of a novel mouse gene, meg1, during the meiotic cell cycle. *Cell Growth Differ.* 1992;3(8):495-505.
37. Zhang Z, Shen X, Gude DR, et al. MEIG1 is essential for spermiogenesis in mice. *Proc Natl Acad Sci U S A.* 2009;106(40):17055-17060. doi:[10.1073/pnas.0906414106](https://doi.org/10.1073/pnas.0906414106)
38. Sheffer R, Gur M, Brooks R, et al. Biallelic variants in AGTPBP1, involved in tubulin deglutamylation, are associated with cerebellar degeneration and motor neuropathy. *Eur J Hum Genet.* 2019;27(9):1419-1426. doi:[10.1038/s41431-019-0400-y](https://doi.org/10.1038/s41431-019-0400-y)
39. Keller N, Paketci C, Altmueller J, et al. Genomic variants causing mitochondrial dysfunction are common in hereditary lower motor neuron disease. *Hum Mutat.* 2021;42(4):460-472. doi:[10.1002/humu.24181](https://doi.org/10.1002/humu.24181)
40. Mullen RJ, Eicher EM, Sidman RL. Purkinje cell degeneration, a new neurological mutation in the mouse. *Proc Natl Acad Sci U S A.* 1976;73(1):208-212. doi:[10.1073/pnas.73.1.208](https://doi.org/10.1073/pnas.73.1.208)
41. Landis SC, Mullen RJ. The development and degeneration of Purkinje cells in pcd mutant mice. *J Comp Neurol.* 1978;177(1):125-143. doi:[10.1002/cne.901770109](https://doi.org/10.1002/cne.901770109)
42. Chakrabarti L, Neal JT, Miles M, et al. The Purkinje cell degeneration 5J mutation is a single amino acid insertion that destabilizes Nna1 protein. *Mamm Genome.* 2006;17(2):103-110. doi:[10.1007/s00335-005-0096-x](https://doi.org/10.1007/s00335-005-0096-x)
43. Audebert S, Desbruyeres E, Gruszczynski C, et al. Reversible polyglutamylation of alpha- and beta-tubulin and microtubule dynamics in mouse brain neurons. *Mol Biol Cell.* 1993;4(6):615-626. doi:[10.1091/mbc.4.6.615](https://doi.org/10.1091/mbc.4.6.615)
44. Janke C, Rogowski K, Wloga D, et al. Tubulin polyglutamylase enzymes are members of the TTL domain protein family. *Science.* 2005;308(5729):1758-1762. doi:[10.1126/science.1113010](https://doi.org/10.1126/science.1113010)
45. Kalinina E, Biswas R, Berezniuk I, Hermoso A, Aviles FX, Fricker LD. A novel subfamily of mouse cytosolic carboxypeptidases. *FASEB J.* 2007;21(3):836-850. doi:[10.1096/fj.06-7329com](https://doi.org/10.1096/fj.06-7329com)
46. Pleuger C, Lehti MS, Dunleavy JE, Fietz D, O'Bryan MK. Haploid male germ cells—the grand Central Station of protein transport. *Human Reproduction Update.* 2020;26(4):474-500. doi:[10.1093/humupd/dmaa004](https://doi.org/10.1093/humupd/dmaa004)

SUPPORTING INFORMATION

Additional supporting information can be found online in the Supporting Information section at the end of this article.

How to cite this article: Lin Y-H, Wang Y-Y, Lai T-H, et al. Deleterious genetic changes in *AGTPBP1* result in teratozoospermia with sperm head and flagella defects. *J Cell Mol Med.* 2024;28:e18031. doi:[10.1111/jcmm.18031](https://doi.org/10.1111/jcmm.18031)